Alteration Analysis of Bone Marrow Mesenchymal Stromal Cells from De Novo Acute Myeloid Leukemia Patients at Diagnosis

Laura Desbourdes,[1] Joaquim Javary,[1] Thomas Charbonnier,[2] Nicole Ishac,[1]
Jerome Bourgeais,[1] Aurore Iltis,[2,3] Jean-Claude Chomel,[4,5] Ali Turhan,[6,7] Fabien Guilloton,[8]
Karin Tarte,[8–10] Marie-Veronique Demattei,[11] Elfi Ducrocq,[1] Florence Rouleux-Bonnin,[1]
Emmanuel Gyan,[1,3] Olivier Hérault,[1,2,10] and Jorge Domenech[1,2,10]

Bone marrow (BM)-derived mesenchymal stromal cells (MSCs) frequently display alterations in several hematologic disorders, such as acute lymphoid leukemia, acute myeloid leukemia (AML), and myelodysplastic syndromes. In acute leukemias, it is not clear whether MSC alterations contribute to the development of the malignant clone or whether they are simply the effect of tumor expansion on the microenvironment. We extensively investigated the characteristics of MSCs isolated from the BM of patients with de novo AML at diagnosis (L-MSCs) in terms of phenotype (gene and protein expression, apoptosis and senescence levels, DNA double-strand break formation) and functions (proliferation and clonogenic potentials, normal and leukemic hematopoiesis-supporting activity). We found that L-MSCs show reduced proliferation capacity and increased apoptosis levels compared with MSCs from healthy controls. Longer population doubling time in L-MSCs was not related to the AML characteristics at diagnosis (French–American–British type, cytogenetics, or tumor burden), but was related to patient age and independently associated with poorer patient outcome, as was cytogenetic prognostic feature. Analyzing, among others, the expression of 93 genes, we found that proliferative deficiency of L-MSCs was associated with a perivascular feature at the expense of the osteo-chondroblastic lineage with lower expression of several niche factors, such as *KITLG*, *THPO*, and *ANGPT1* genes, the cell adhesion molecule *VCAM1*, and the developmental/embryonic genes, *BMI1* and *DICER1*. L-MSC proliferative capacity was correlated positively with *CXCL12*, *THPO*, and *ANGPT1* expression and negatively with *JAG1* expression. Anyway, these changes did not affect their in vitro capacity to support normal hematopoiesis and to modify leukemic cell behavior (protection from apoptosis and quiescence induction). Our findings indicate that BM-derived MSCs from patients with newly diagnosed AML display phenotypic and functional alterations such as proliferative deficiency that could be attributed to tumor progression, but does not seem to play a special role in the leukemic process.

Keywords: hematopoiesis, microenvironment, mesenchymal stromal cells, niche, acute myeloid leukemia

Introduction

DYSFUNCTIONS OF THE hematopoietic system can lead to the emergence of malignancies such as acute myeloid leukemias (AMLs), which involve the hematopoietic stem cell (HSC) compartment. These disorders originating from bone marrow (BM) are characterized by clonal proliferation of cells having lost more or less their maturation capacities associated with a dramatic suppression of normal polyclonal hematopoiesis [1]. The mechanisms underlying this suppression are not yet completely elucidated. Indeed, it can be observed also in the case of limited leukemic cell infiltration and therefore it cannot be explained only by BM expansion of tumor cells. The heterogeneity of the AML cell population is now well

[1]CNRS UMR 7292, LNOx Team, François Rabelais University, Tours, France.
Departments of [2]Biological Hematology and [3]Hematology and Cell Therapy, University Hospital of Tours, Tours, France.
[4]INSERM U935, University of Poitiers, Poitiers, France.
[5]Department of Biological Oncology, University Hospital of Poitiers, Poitiers, France.
[6]INSERM U935, University of Paris-Sud 11, Paris, France.
[7]Department of Hematology, University Hospitals of Paris-Sud, Le Kremlin Bicêtre, France.
[8]INSERM U917, University of Rennes 1, Rennes, France.
[9]Department of Immunology, Cellular Therapy and Hematopoiesis, University Hospital of Rennes, Rennes, France.
[10]CNRS GDR 3697, MicroNiT National Network, Tours, France.
[11]CNRS UMR 7292, Telomeres and Genome Stability Team, François Rabelais University, Tours, France.

established and includes a rare subpopulation named leukemic stem cells (LSCs) that are regulated by the BM stromal compartment [2–4]. LSCs can maintain and promote tumor cell propagation and favor resistance to treatment [5].

Mesenchymal stromal cells (MSCs) are the main cellular component of the hematopoietic niche [6–8] in the BM, a specialized microenvironment site that controls self-renewal and quiescence of HSCs. MSCs are multipotent cells that give rise to vascular smooth muscle cells, adipocytes, osteoblasts of the BM, and also chondroblasts. Alterations of the BM stromal cell compartment have been shown in de novo AML, including a reduction in the number of fibroblasts and adipocytes and a decreased growth capacity [9–14]. However, it is not yet evident if MSC long-term hematopoietic-supporting activity in AML at diagnosis is intrinsically impaired [12] or not [10]. Otherwise, several recent reports have highlighted the abnormal MSC function in chronic preleukemic diseases such as myelodysplastic syndromes (MDSs) [15–17] in contrast to chronic myelogenous leukemia (CML) [18,19].

In primary AML, it remains to be clarified whether the observed microenvironmental alterations contribute to the development of the malignant clone or are simply the consequence of cancer cell proliferation at the onset of the disease. Some reports have shown that leukemic cells alter the hematopoietic function of the BM microenvironment by disrupting the hematopoietic niches [20] and by inducing sympathetic neuropathy that increases BM leukemic infiltration [21]. In addition, the microenvironment contribution to leukemia progression has been suggested by the occurrence of hematopoietic malignancies derived from donor cells in recipients of allogeneic HSC transplants [22,23] and was demonstrated in animal models [24–26].

The present study investigated the relationship between the phenotype (extensively analyzed) and function of MSCs isolated from the BM of patients with newly diagnosed de novo AML (L-MSCs). As in previous reports, we found that L-MSCs often display a proliferative deficiency. In this study, we show that this abnormality, correlated with the patient's age, is not related to AML characteristics at diagnosis [French–American–British (FAB) type, cytogenetics, or tumor burden] and is independently associated with poorer patient outcome. Analyzing, among others, the expression of 93 genes, we found that proliferative deficiency of L-MSCs was associated with a perivascular feature at the expense of the osteochondroblastic lineage with lower expression of several niche factors, such as *KITLG*, *THPO*, and *ANGPT1*, the cell adhesion molecule *VCAM1*, and the developmental/embryonic genes, *BMI1* and *DICER1*. L-MSC proliferative capacity correlated positively with *CXCL12*, *THPO*, and *ANGPT1* expression and negatively with *JAG1* expression. Nevertheless, these changes, probably induced by tumor expansion, did not affect the in vitro capacity of MSCs to support normal hematopoiesis and to modify the leukemic cell biology (protection from apoptosis and quiescence induction).

Materials and Methods

Patients and normal controls

All patients included in this study (12 males and 7 females) had de novo AML followed at the Department of Clinical Hematology, University Hospital, Tours, France, and gave their informed consent for cell banking according to the Declaration of Helsinki, and the study was approved by the French Ministry of Higher Education and Research (authorization number No. DC-2008-308). BM samples were collected at diagnosis for MSCs and contained 87% of blast cells (median value), while peripheral blood (PB) leukocyte count was in median 57 g/L. Patients had a median age of 48 years at the time of BM aspiration. According to the FAB classification, AMLs were classified as AML-M0/1 ($n = 10$ patients), AML-M3 ($n = 3$), and AML-M4/5 ($n = 6$). The patients' clinical data are reported in Supplementary Table S1 (Supplementary Data are available online at www.liebertpub.com/scd). In parallel, BM MSCs from normal controls without any hematological disorder (seven males and three females; median age: 59.5 years) were isolated. They were informed and consenting patients underwent orthopedic surgery (Orthopedic Surgery Department, Trousseau Hospital, Tours, France), or for brain-dead organ donors, just before organ harvesting (protocol approved by the French Biomedicine Agency, no. PFS10-007), the family provided the written informed consent.

BM-derived MSC expansion and clonogenic capacity

BM cells obtained by iliac crest or sternal aspiration were centrifuged and propagated in expansion medium.

Proliferation capacity. To measure MSC proliferation capacity, the population doubling time (PDT) was estimated at each passage and by flow cytometry using the carboxyfluorescein succinimidyl ester (CFSE).

Colony-forming unit-fibroblast assay. MSC clonogenic capacity was assessed by seeding 10–40/cm^2 adherent cells in T-25 flasks. At day 10, cell clusters containing more than 50 cells were scored as colony-forming unit-fibroblast (CFU-F) colonies using an inverted microscope. Details are provided in the Supplementary Methods section in Supplementary Data.

BM-derived MSC differentiation potential

Multipotency of adherent MSCs was evaluated by inducing differentiation toward the adipogenic, osteogenic, and chondrogenic lineages. Detailed information is available in the Supplementary Methods section in Supplementary Data.

MSC cycle analysis

The percentage of detached MSCs in the G0, G1, or S/G2/M phase of the cell cycle was determined by flow cytometry after staining with 7-AAD and an anti-human KI67-*Alexa* Fluor 488-conjugated antibody, as previously described [27]. Additionally, expression of the cell cycle proteins, cyclin D1, p21, p27, and p53, in MSCs was investigated by western blotting. Details are provided in the Supplementary Methods section in Supplementary Data.

MSC damage evaluation

MSC apoptosis. Cell apoptosis rate was assessed by flow cytometry using the Annexin V-fluorescein isothiocyanate (FITC)/7-AAD Kit (Beckman Coulter) [28]. Late apoptosis was assessed in ethanol-permeabilized cells after 7-AAD staining to detect hypoploid nuclei (sub-G1 peak).

Cell senescence. Senescence rates were assessed on adherent layers of MSCs at 70% confluence, using the Senescence Cells Histochemical Staining Kit (Sigma Aldrich).

MSC telomere length. DNA from MSCs was extracted with the Genomic DNA from Tissue kit (Macherey-Nagel Dueren). MSC telomere length was measured by Southern blot analysis of terminal restriction fragments as previously described [29].

Reactive oxygen species production. The amount of intracellular reactive oxygen species (ROS) was evaluated in trypsin/ethylenediaminetetraacetic acid (EDTA)-harvested MSCs by CM-H2DCFDA staining (Molecular Probes).

DNA double-strand break formation. The presence of DNA double-strand breaks (DSBs) was assessed in detached MSCs by staining with an FITC-conjugated antibody against phospho-histone H2AX (Ser139) (γH2AX) (clone JBW301, IgG1; EMD Millipore) after ethanol permeabilization. Details are provided in the Supplementary Methods section in Supplementary Data.

MSC gene and protein expression related to niche function

Reverse transcriptase–quantitative polymerase chain reaction analysis. We evaluated 93 genes (Supplementary Table S2) by TaqMan reverse transcriptase–quantitative polymerase chain reaction analysis (RT-qPCR).

Cytokine concentration in MSC supernatants. Cytokine levels were measured in supernatants of subconfluent MSCs at P2 by enzyme-linked immunosorbent assay (ELISA) using the Quantikine Human Immunoassays (R&D Systems) for stromal cell-derived factor-1 alpha (SDF-1α), angiopoietin-1 (ANG-1), thrombopoietin (TPO), and stem cell factor (SCF), according to the manufacturer's recommendations.

Immunophenotype analysis. Membrane antigen expression was assessed by flow cytometry after direct (for CD45, CD14, CD34, CD309, CD73, CD90, CD105, CD49e, and CD146) or indirect (for CD106) staining of trypsin/EDTA-detached subconfluent MSCs at P2.

Immunofluorescence. The MSC expression of fibronectin, alpha smooth muscle actin (ASMA), and nestin was observed by immunofluorescence staining. Details are provided in the Supplementary Methods section in Supplementary Data.

MSC hematopoietic-supporting activity assessed by Dexter-type long-term cultures

Confluent MSCs cultured in T-25 flasks were irradiated and recharged with normal peripheral CD34^{pos} cells in hydrocortisone-supplemented Myelocult® medium (H5100; StemCell Technologies) as described in the Supplementary Methods section in Supplementary Data. Hematopoietic progenitor cell (HPC) production was assessed weekly for 5 weeks.

MSC leukemic cell supporting activity

MSC influence on leukemic cell behavior was evaluated by coculturing MSCs from patients with AML-M0/1 (L-MSC) or from controls (N-MSC) with KG1a cells for 3 days ($n=6$/each group) or with primary blast cells (AML-M0/1) in heterologous or autologous settings for 2 days ($n=4$ for each group and each setting). Controls were KG1a cells ($n=3$) and primary blast cells ($n=4$) grown without MSCs.

Apoptosis rate [28], cell cycle distribution [27], and DNA DSBs in leukemic cells (CD45^{pos} cell fraction) grown with or without MSCs were assessed by flow cytometry. Detailed information is available in the Supplementary Methods section in Supplementary Data.

Statistical analyses

N-MSCs and L-MSCs were compared using the non-parametric Mann–Whitney test in all experiments, except for cocultures of MSCs with leukemic cells where paired values were analyzed with the nonparametric Wilcoxon test. Correlations between quantitative values were evaluated by the Spearman rank test. Multivariate analysis was performed using the multiple stepwise regression test. Differences were considered significant when $P < 0.05$.

Results

Adherent cells from BM of patients with AML exhibit characteristics of multipotent MSCs

To characterize the adherent BM cells isolated from patients with newly diagnosed AML and from controls, the expression of hematopoietic (CD14, CD34, and CD45) and endothelial (CD31 and CD309) markers was assessed at P2 and found to range between <1% and 5%. CD45^{neg} cells from patients and controls expressed classical MSC markers (CD73, CD90, and CD105) (Fig. 1A) and could differentiate into adipogenic, osteogenic, and chondrogenic lineages (Fig. 1B). These results indicate that BM-derived adherent cells from both patients with AML (L-MSCs) and normal controls (N-MSCs) meet all the criteria to be considered MSCs [30] and show no obvious different characteristics.

The proliferation capacity of MSCs isolated from patients with AML is decreased and is independently related to patient outcome

MSC proliferation capacity was assessed by calculating the PDT, which was significantly longer in L-MSC than in N-MSC samples ($P < 0.01$; Fig. 2A) with wide interindividual variation. Conversely, the clonogenic potential, evaluated with the CFU-F assay in MSC samples at P2, tended to be lower in L-MSC than in N-MSC samples ($P = 0.16$; Fig. 2B), while an inverse correlation was found between CFU-F and PDT values ($\rho = 0.79$, $P < 0.001$). Interestingly, L-MSCs isolated at diagnosis from patients who experienced treatment failure or early relapse (Supplementary Table S1) had significantly higher PDT values at P2 than L-MSCs from patients remaining in complete remission (Fig. 2C; $P < 0.01$). No significant correlation was found between PDT and sex, FAB type, PB leukoblast count, BM leukoblast percentage, and cytogenetic prognostic feature at diagnosis. However, PDT correlated with patient age, as expected ($\rho = 0.57$; $P < 0.05$). The lower L-MSC proliferation capacity was confirmed by the decreased difference between the mean fluorescent intensity values of CFSE staining at 24 and 96 h in L-MSC cultures compared with controls ($P < 0.05$; Fig. 2D). However, no difference in the cell cycle distribution between N-MSC and L-MSC samples was detected by flow cytometry analysis after 7-AAD and KI-67 staining (Supplementary Fig. S1A).
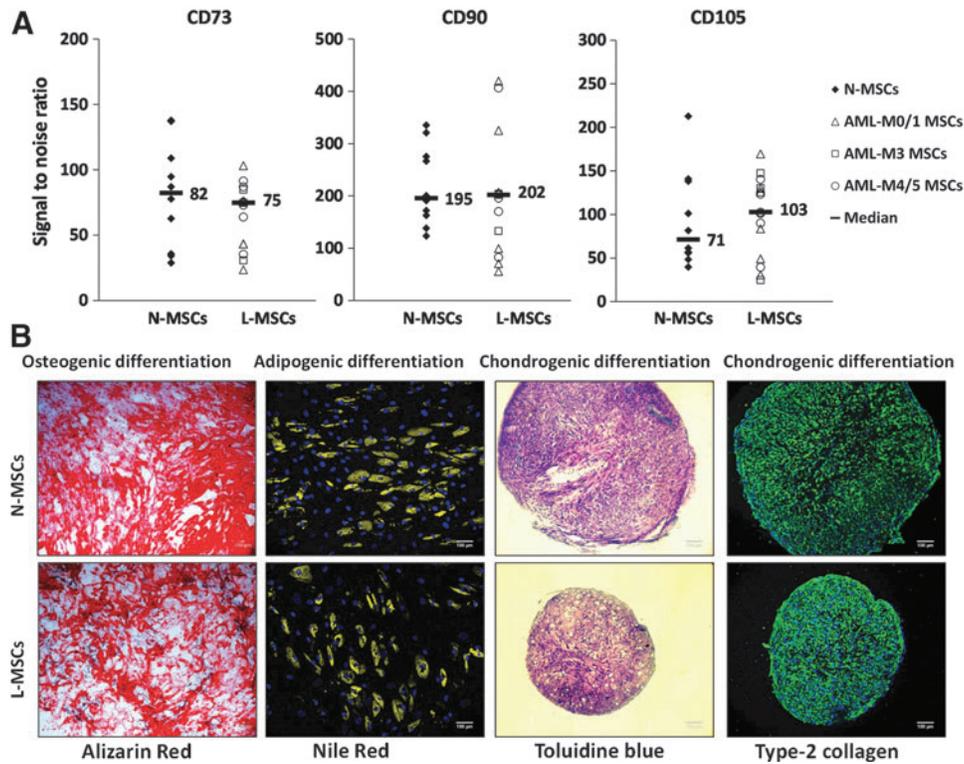
FIG. 1. Adherent cells from bone marrow of AML patients and normal controls display typical mesenchymal characteristics. **(A)** Expression of classical MSC markers measured by flow cytometry in adherent $CD45^{neg}$ cells from patients with AML (L-MSCs; $n = 15$) and controls (N-MSCs; $n = 10$). Values are the signal-to-noise ratios determined by calculating the ratio of the median fluorescent intensities for specific antibody and isotype-matched control antibody. *Black diamonds*, individual N-MSC samples; *triangles*, individual L-MSC samples from patients with AML-M0/1; *squares*, individual L-MSC samples from patients with AML-M3; *circles*, individual L-MSC samples from patients with AML-M4/5. *Horizontal bars* represent the medians. **(B)** L-MSCs ($n = 14$) have the same differentiation potential as N-MSCs ($n = 10$). Representative microphotographs of osteogenic, adipogenic, and chondrogenic differentiation of MSCs from one control (N-MSCs) and one patient with AML (L-MSCs). For osteogenic and adipogenic differentiation, confluent cells were exposed to a specific induction medium for 2 weeks. The presence of calcium deposits in osteocytes was revealed by Alizarin Red staining. Cellular neutral lipid vacuoles were stained with Nile Red (*yellow*). Chondrogenic differentiation was performed on cell pellets. After 3-week induction, the presence of glycosaminoglycans was revealed by toluidine blue staining and of type II collagen by immunofluorescence (*green*). Cell nuclei were stained with DAPI (*blue*). Scale bars = 100 μm. MSC, mesenchymal stromal cell; AML, acute myeloid leukemia; DAPI, 4′,6-diamidino-2-phenylindole.

Accordingly, cell cycle regulatory proteins (cyclin D1, p21, p27, and p53) were expressed at comparable levels in L-MSC and N-MSC cultures (Supplementary Fig. S1B, C).

Flow cytometry analysis after Annexin V/7-AAD staining revealed higher rates of early apoptotic cells ($7-AAD^{neg}$/Annexin V^{pos}) ($P < 0.05$; Fig. 3A) and also necrotic cells ($7-AAD^{pos}$/Annexin V^{pos}) ($P < 0.05$; data not shown) in L-MSC than in N-MSC cultures at P2. Likewise, when only late apoptosis was investigated, after 7-AAD staining, L-MSCs showed an increase in the percentage of hypoploid cells (sub-G1 phase) ($P < 0.05$; Fig. 3B). Similar results were obtained when the death rate was measured with trypan blue exclusion staining ($P < 0.05$). However, increased levels of DNA DSBs, cell senescence, telomere length changes, and intracellular ROS levels could not be detected in L-MSCs when evaluated at the end of the second passage (Supplementary Fig. S2A–D). It should be noted that senescence values in L-MSCs were particularly dispersed (Supplementary Fig. S2B).

To investigate whether L-MSC characteristics (PDT, clonogenic potential, senescence levels) might indepen-

dently influence patient outcome (complete remission or disease progression), a multivariate stepwise regression analysis was carried out by integrating these variables with patient and disease characteristics (sex, age, PB leukoblast count, BM leukoblast percentage, FAB type, and cytogenetic prognostic feature at diagnosis). The only two independent prognostic factors found for patient outcome ($P < 0.01$) were cytogenetic prognostic value ($F = 6.11$) and especially PDT ($F = 13.63$).

The expression of niche factors is downregulated in MSCs from AML patients

To further characterize L-MSCs, the expression of 95 genes (including the control genes *B2M* and *EIF2B1*; Supplementary Table S2) was evaluated in L-MSCs and N-MSCs by RT-qPCR. Although 11 genes could not be amplified (*CCL19*, *COL2A1*, *CXCL9*, *GPX2*, *GPX5*, *IHH*, *LPL*, *PROM1*, *SHH*, *TERT*, and *WNT3A*), the transcriptional profile of the other genes, including 22 niche-related genes,
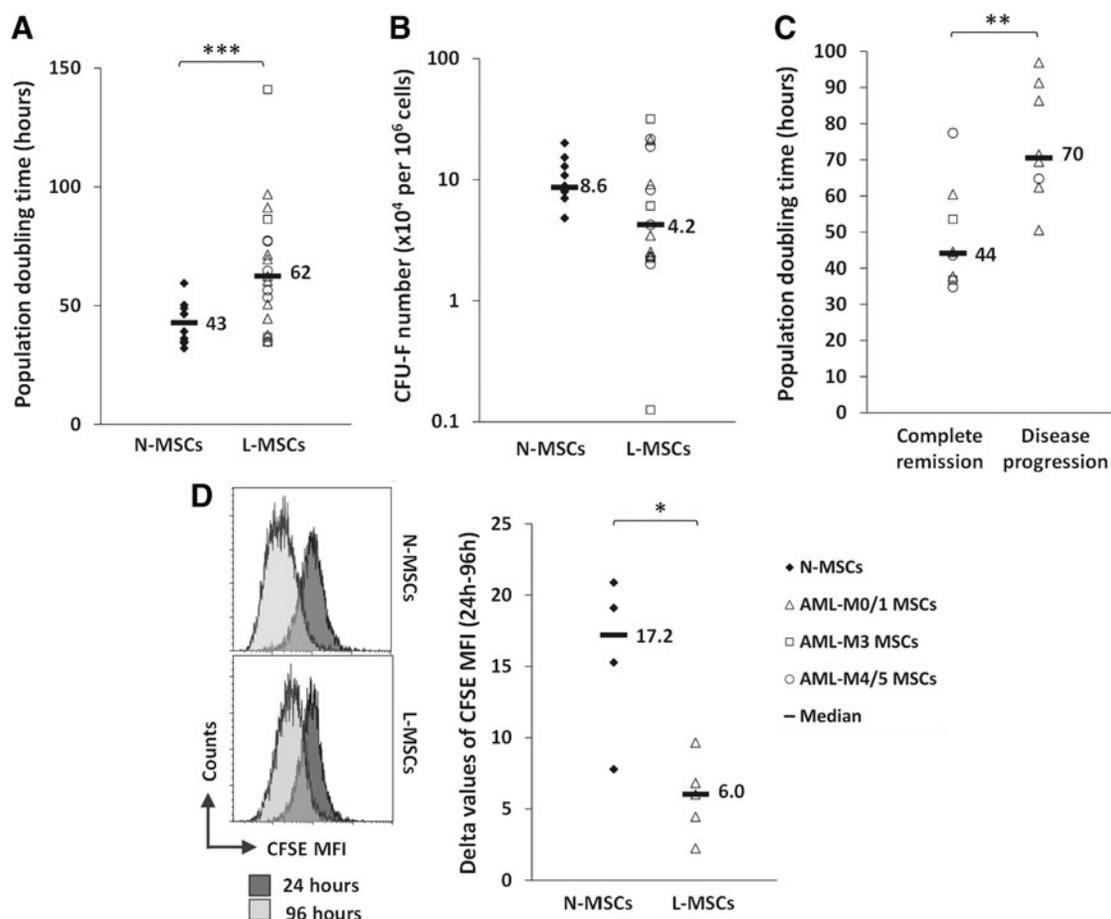
FIG. 2. MSCs from AML patients (L-MSCs) have lower proliferative potential than MSCs from normal individuals (N-MSCs). **(A)** Cell proliferation capacity determined by PDT of L-MSCs ($n = 19$) and N-MSCs ($n = 10$). **(B)** Clonogenic capacity of L-MSCs ($n = 15$) and N-MSCs ($n = 10$) evaluated by CFU-F assay. **(C)** PDT of L-MSCs at P2 isolated from patients in complete remission ($n = 8$) or with disease progression ($n = 11$). **(D**, *left*) Representative images of flow cytometry analysis of CFSE MFI after 24 (*dark gray*) and 96 (*light gray*) h of staining. The difference between these two MFI values (ΔMFI) reflects the cell proliferative potential over 72 h. **(D**, *right*) ΔMFI values in L-MSCs ($n = 5$) and N-MSCs ($n = 4$). For symbols, see legend in Fig. 1. *Horizontal bars* represent the medians. *$P < 0.05$; **$P < 0.01$; ***$P < 0.005$. PDT, population doubling time; CFU-F, colony-forming unit-fibroblast; MFI, mean fluorescence intensity.

showed decreased expression ($P < 0.05$) of genes encoding secreted cytokines, such as ANG-1 (*ANGPT1*), SCF (*KITLG*), and TPO (*THPO*), in L-MSCs compared with N-MSCs (Fig. 4A), while the expression of the genes encoding SDF-1α (*CXCL12*), FLT3-Ligand (*FLT3LG*), and Jagged 1 (*JAG1*) was similar between groups. Conversely, the expression of genes encoding the adhesion molecules, integrin alpha 5 (CD49e/*ITGA5*) ($P < 0.01$) and melanoma cell adhesion molecule (CD146/*MCAM*) ($P < 0.05$), was increased in L-MSCs compared with N-MSCs, whereas the genes encoding VCAM-1 (CD106/*VCAM1*) and integrin alpha 6 (CD49F/*ITGA6*) were downregulated ($P < 0.05$). Gene expression of MSC markers, such as ASMA (*ACTA2*), nestin (*NES*), and NGF receptor (CD271/*NGFR*), and of extracellular matrix molecules, such as fibronectin 1 (*FN1*), collagen 1A1 (*COL1A1*), 4A1 (*COL4A1*), and osteopontin (OPN/ *SPP1*), was not significantly different between groups. Among the other 60 genes (Supplementary Fig. S3A, B), genes involved in the osteogenic lineage, such as osteo-calcin (OCN/*BGLAP*) and *RUNX2*, or in the chondrogenic

lineage (*COL10A1*) were downregulated in L-MSCs compared with N-MSCs ($P < 0.05$), whereas *BMP1* was upregulated ($P < 0.05$) and no change was observed in *PPARG*, an adipogenic lineage gene. *RUNX2* and *BMP1* expression was inversely correlated ($\rho = -0.61$; $P < 0.05$). The expression of developmental/embryonic genes, such as *OCT4/ POU5F1*, *SOX2*, and *NANOG*, was unchanged, but for *BMI1* that was downregulated in L-MSCs ($P < 0.05$) as found for *DICER1*, a gene encoding a ribonuclease involved in the RNA interference pathway. However, the reduction of *KITLG*, *ANGPT1*, and *THPO* gene expression was not confirmed by ELISA analysis of secreted niche factors in L-MSC and N-MSC supernatants (Fig. 4B–E). Likewise, increased CD49e and CD146 gene expression in L-MSCs was only associated with a tendency to increased membrane protein expression quantified by flow cytometry (Fig. 4F). Nevertheless, CD146 gene expression positively correlated with CD49e protein expression ($\rho = 0.74$; $P < 0.01$). It is noteworthy that CD146 protein expression level also positively correlated with BM leukoblast percentage in L-MSCs
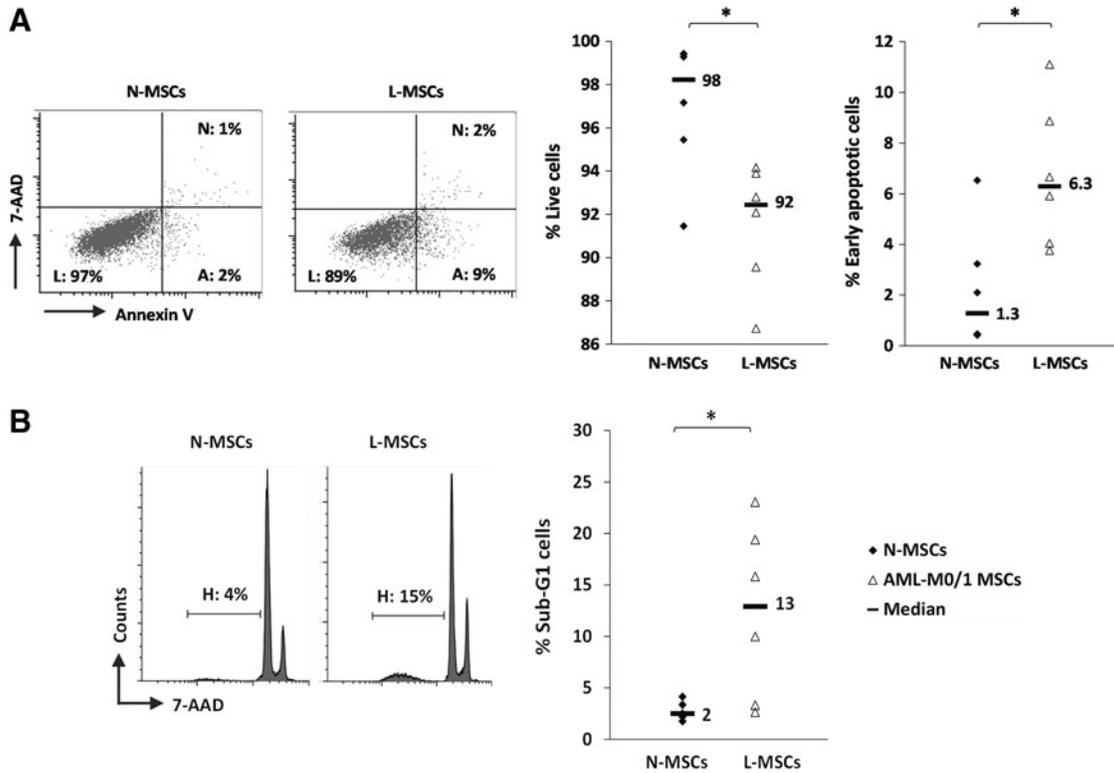
FIG. 3. L-MSCs show higher apoptosis rates than N-MSCs. (**A**, *left*) Representative images of flow cytometry analysis of early apoptosis in MSCs. (**B**, *right*) Quantification of MSC apoptosis analysis expressed in percentage of live (7-AAD^{neg}/ Annexin V^{neg} cells) and early apoptotic (7-AAD^{neg}/Annexin V^{pos} cells) cells for L-MSCs ($n=6$) and N-MSCs ($n=6$). (**B**, *left*) Representative flow cytometry analysis of late apoptosis in MSCs fixed and permeabilized before 7-AAD staining showing the presence of hypoploid (H) cells (sub-G1). (**B**, *right*) Percentage of hypoploid cells in L-MSC ($n=6$) and N-MSC cultures ($n=6$). *Black diamonds*, individual N-MSC samples; *triangles*, individual L-MSC samples from patients with AML-M0/1. *Horizontal bars* represent the medians. *$P<0.05$.

($\rho=0.80$; $P<0.001$) and inversely correlated with the patient age considering MSCs from leukemic patients, normal controls, or both ($\rho=0.63$; $P<0.001$). CD106 protein (VCAM-1) expression was meanwhile significantly decreased in L-MSCs compared with N-MSCs ($P<0.05$; Fig. 4G), in accordance with the mRNA findings (Fig. 4A). No qualitative or quantitative differences between L-MSCs and N-MSCs in the extracellular matrix deposition of fibronectin and the intracellular expression of the cytoskeleton proteins ASMA and nestin were observed by immunofluorescence analysis (Fig. 5), according to the gene expression data (Fig. 4A).

Considering the wide variations found in L-MSC growth capacity, a relationship between this capacity and L-MSC phenotype was investigated. Thus, longer PDT was associated with lower expression of *RUNX2* ($\rho=-0.64$; $P<0.05$), *COL10A1* ($\rho=-0.64$; $P<0.05$), *THPO* ($\rho=-0.69$; $P<0.05$), less secreted CXCL12 ($\rho=-0.69$; $P<0.05$), and with higher expression of *BMP1* ($\rho=0.75$; $P<0.01$), *ITGA5* ($\rho=0.90$; $P<0.001$), and *JAG1* ($\rho=0.69$; $P<0.05$). Same correlations were also found for lower clonogenicity (CFU-F) with lower expression not only of *RUNX2* ($\rho=0.67$; $P<0.05$), *COL10A1* ($\rho=0.80$; $P<0.01$), *THPO* ($\rho=0.63$; $P<0.05$), and *CXCL12* ($\rho=0.62$; $P<0.05$) [as for secreted CXCL12 ($\rho=0.64$; $P<0.05$)] but also *ANGPT1* ($\rho=0.64$; $P<0.05$) and with higher expression of *BMP1* ($\rho=-0.57$; $P=0.05$), *ITGA5* ($\rho=-0.65$; $P<0.05$), and *JAG1* ($\rho=-0.72$; $P<0.01$).

Moreover, increased level of senescence was associated with lower expression of *RUNX2* ($\rho=-0.81$; $P<0.01$), *COL10A1* ($\rho=-0.82$; $P<0.01$), *ITGA4* ($\rho=-0.75$; $P<0.01$), *DICER1* ($\rho=-0.72$; $P<0.05$), *BMI1* ($\rho=-0.70$; $P<0.05$), and especially *ANGPT1* ($\rho=-0.88$; $P<0.001$). Senescence entry also correlated with lower clonogenicity of L-MSCs ($\rho=-0.80$; $P<0.01$). The existence of a strong positive relationship between gene expression of *DICER1* and *BMI1* ($\rho=0.97$; $P<0.00001$) is noteworthy.

MSCs from patients with AML retain normal hematopoietic supportive function

The hematopoiesis-supporting capacity of confluent L-MSCs and N-MSCs was tested by using Dexter-type long-term cocultures recharged with normal CD34^{pos} cells for 5 weeks. To limit patient heterogeneity, we focused this study on L-MSCs from patients with AML-M0/1 (L-MSCs a, b, c, d). Weekly assessment of the HPC number in supernatants was not significantly different in L-MSC and N-MSC cocultures (Fig. 6A). Similar findings were obtained when the total HPC production from adherent and nonadherent cell fractions was evaluated at the end of week 5 (Fig. 6B). The microscopic visualization of cobblestone areas in both L-MSC and N-MSC cocultures at week 5 also supported these results (Fig. 6C). The normal hematopoietic supportive function of L-MSCs cannot be explained only by biased
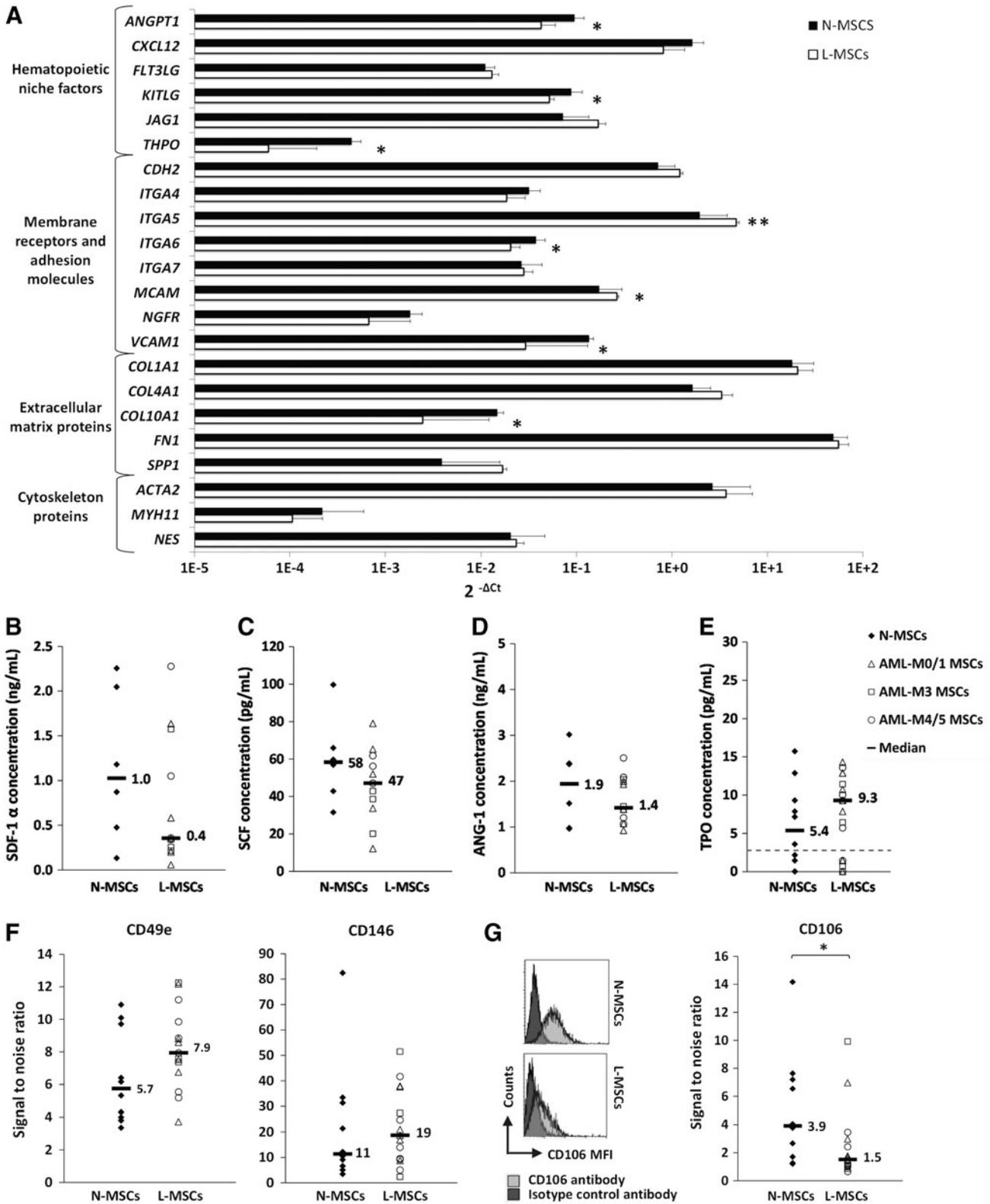
FIG. 4. The expression of niche factors is altered in L-MSCs. **(A)** Transcriptional profile of 22 niche-related genes in L-MSCs ($n=12$) and N-MSCs ($n=6$). Values represent the relative expression ($2^{-\Delta Ct}$ value) of each gene normalized to a computed endogenous control (aggregated median of *B2M* and *EIF2B1* expression). Bars, medians; and error bars, semi-interquartile ranges. **(B–E)** Protein expression of the secreted niche factors SDF-1α, SCF, and ANG-1 measured by enzyme-linked immunosorbent assay in supernatants from L-MSC ($n=12$) and N-MSC ($n=6$) samples; for TPO: L-MSCs ($n=19$) and N-MSCs ($n=10$). **(F, G)** Expression levels of membrane receptors and adhesion molecules measured by flow cytometry in L-MSC ($n=15$) and N-MSC ($n=10$) samples. Signal-to-noise ratio: ratio between the median fluorescence intensities (MFIs) for the specific and isotype-matched control antibodies. CD49e (integrin alpha 5) and CD146 (MCAM) expression was evaluated by direct staining **(F)** and CD106 (VCAM-1) by indirect staining **(G)**. For symbols, see legend in Fig. 1. *Horizontal bars* represent the medians. *$P<0.05$; **$P<0.01$. SDF-1α, stromal cell-derived factor-1 alpha; SCF, stem cell factor; ANG-1, angiopoietin-1; TPO, thrombopoietin.
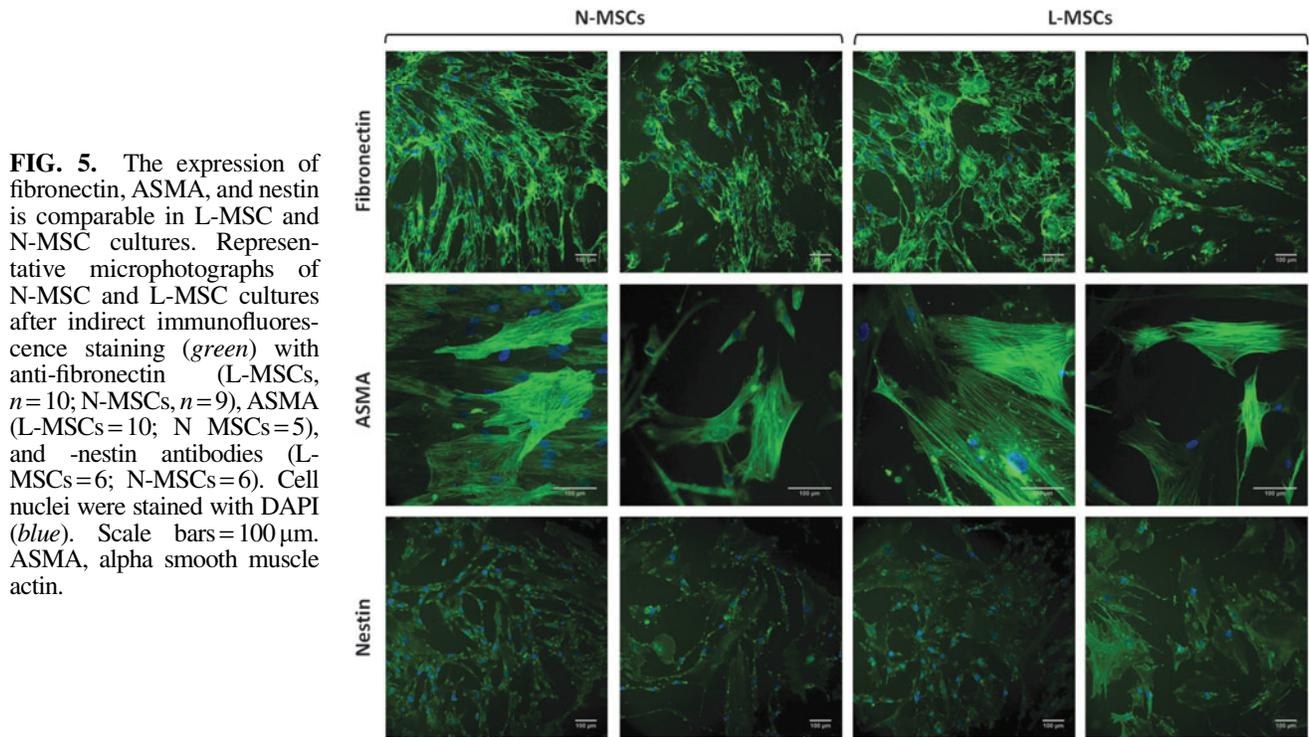
FIG. 5. The expression of fibronectin, ASMA, and nestin is comparable in L-MSC and N-MSC cultures. Representative microphotographs of N-MSC and L-MSC cultures after indirect immunofluorescence staining (*green*) with anti-fibronectin (L-MSCs, $n = 10$; N-MSCs, $n = 9$), ASMA (L-MSCs = 10; N MSCs = 5), and -nestin antibodies (L-MSCs = 6; N-MSCs = 6). Cell nuclei were stained with DAPI (*blue*). Scale bars = 100 μm. ASMA, alpha smooth muscle actin.
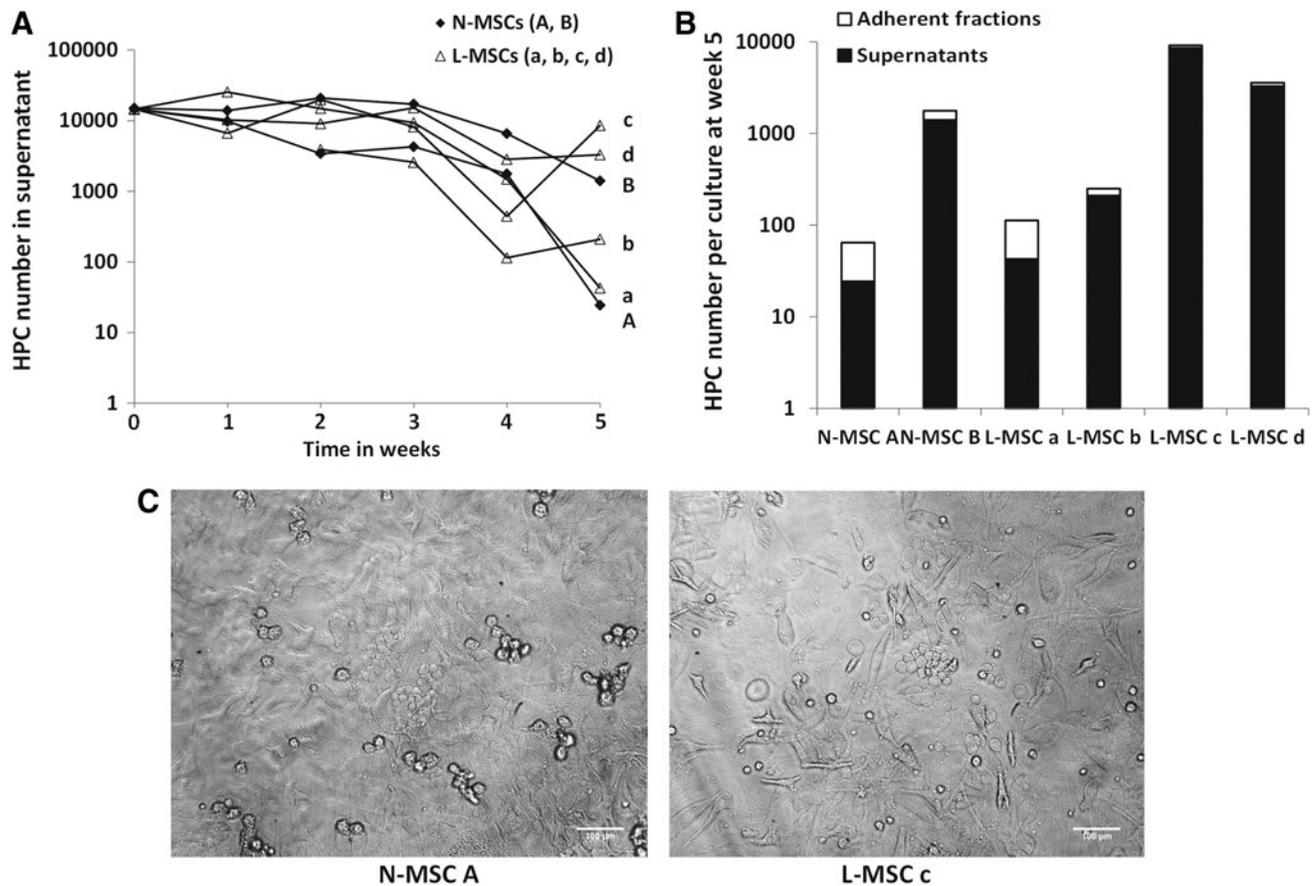

FIG. 6. L-MSCs show normal hematopoietic supportive functions. (**A**, **B**) Dexter-type long-term cultures were performed in which CD34+ cells were cocultured on confluent layers of 10-Gy irradiated MSCs from patients with AML (L-MSCs; a, b, c, d) or from controls (N-MSCs; A, B) for 5 weeks. HPC production in the coculture supernatants was assessed weekly (**A**), and at the end of week 5, total HPC production was measured in the adherent and nonadherent cell fractions (**B**). (**C**) Cobblestone area formation observed at the end of week 5 in both N-MSC (subject A) and L-MSC (patient c) layers. Scale bars = 100 μm. HPC, hematopoietic progenitor cell.

selection of normal cell layers. Indeed, L-MSC d showed one of the best supporting activities while having one of the longest PDT.

MSCs from patients with AML directly influence the behavior of leukemic cells as observed with normal MSCs

The capacity of L-MSCs and N-MSCs to modify leukemic cell behavior was compared by coculturing MSCs with KG1a cells and primary blast cells (AML-M0/1) in heterologous (hetero) and autologous (auto) settings for 2–3 days. The fraction of adherent leukemic cells was not significantly different in cultures of KG1a or primary blast cells with L-MSCs and N-MSCs, as well as in auto and hetero settings (data not shown). The elevated early apoptosis rate of primary blast cells (7-AAD^{neg}/Annexin V^{pos}) observed in MSC-free cultures was significantly and similarly reduced ($p < 0.05$) when they were cocultured with L-MSCs or N-MSCs (Fig. 7A, B). Similar results were obtained when late apoptosis (cells in sub-G1) was analyzed (data not shown). Again, results were comparable when using auto and hetero L-MSCs. Moreover, cell cycle analysis indicated that the fraction of KG1a cells in G0 (7-AAD^{low}/Ki-67^{neg}) was clearly increased in the presence of both L-MSCs and N-MSCs (Fig. 7C) in the whole KG1a population ($P < 0.01$) and particularly in adherent cells ($P < 0.01$) (Supplementary Fig. S4). Similar results were observed using primary blast cells ($P < 0.05$; Fig. 7D). MSC effect on cell cycle exit of primary blast cells was comparable when cocultured with auto or hetero L-MSCs. Moreover, quiescence of blast cells by direct contact with MSCs (N-MSCs or auto and hetero L-MSCs) was associated with a slight decrease in anti-γH2AX staining (a marker of DNA DSBs) compared with MSC-free cultures ($P < 0.01$) (Fig. 7E), consistent with the previously reported relationship between DNA damage level and cell cycle entry [29].

Discussion

This study shows that MSCs isolated from the BM of patients with newly diagnosed de novo AML display some alterations, including reduced proliferation capacity, increased apoptosis, and decreased expression of several niche-related factors, such as SCF, TPO, ANG-1, and VCAM-1, compared with MSCs from controls. Proliferation deficiency of L-MSCs was not related to AML characteristics at diagnosis (FAB type, cytogenetics, or tumor burden), but was independently associated with poorer patient outcome, as was cytogenetic prognostic feature. This defect was correlated with an MSC perivascular feature at the expense of the osteo-chondroblastic lineage and with lower niche factor and higher JAG1 expression. However, these changes are not sufficient to modify L-MSC in vitro capacity to support normal hematopoiesis and to influence the behavior of leukemic cells in vitro.

The main abnormality detected in L-MSCs was a clear decrease in their proliferative potential, as recently reported in AML [9,10,12–14]. Such proliferation defects have also been described in MSCs from several other hematopoietic disorders, such as acute lymphoblastic leukemia (ALL) [31,32], chronic lymphocytic leukemia (CLL) [33,34], and especially MDS [16,17,35,36]. A slight decrease of their

clonogenic potential (CFU-F) was also observed that was inversely correlated with the PDT values. The mechanisms of MSC proliferation impairment at the onset of leukemia are still unclear. The role of leukemic cells on BM-derived MSC proliferation appears undeniable, as demonstrated by in vitro studies with cell supernatants [12,37] that also are able to inhibit osteoblastic differentiation [12]. A recent report showed a specific influence of leukemic CD34+ cells (compared with normal CD34+ cells) cocultured on N-MSCs by a transcriptomic approach, including down-regulation of cell cycle and related function genes [13]. In vivo studies clearly showed that AML development in mice disrupts the BM microenvironment, resulting in fewer endosteal osteoblasts and more osteoclasts [38], and that osteoblast ablation accelerates CML development [39]. Such changes have been described also in preleukemic disease models [24–26].

Moreover, L-MSC growth impairment can be restored with the repetition of chemotherapy cycles [32] or at diagnosis when most leukemic cells are eliminated by immunoselection of CD105^{pos} MSCs [10]. It has been shown that fragmented DNA released by AML cells may enter MSC nuclei and induce DNA DSBs and cell death [40]. Accordingly, we found increased early and late apoptosis rates in L-MSCs (as reported in CLL [33]), while DNA DSB presence, cell senescence, intracellular ROS production, and telomere length were unchanged. The lack of relationship between decreased MSC proliferative capacity and telomere length has already been reported [41] and is probably due to the use of MSCs after limited passages (P2).

An original data item of our study is the identification of L-MSC proliferative capacity (based on PDT evaluation) as a strong independent prognostic factor for patient outcome (besides cytogenetic prognostic feature, as expected), which was not found for leukemia FAB type or tumor burden. Thus, a longer PDT might highlight the presence of a leukemic clone with a particular toxicity and aggressiveness toward the BM stromal compartment.

L-MSC proliferative deficiency was associated with other abnormal phenotypic features. Particularly, expression of the genes encoding the cytokines ANG-1, SCF, and TPO, as well the adhesion molecule VCAM-1, was downregulated in L-MSCs. This decrease was confirmed for VCAM-1 protein membrane expression. Such results are consistent with a recent report showing that sorted BM stromal cells from a mouse model of AML express lower levels of Vcam1, Cxcl12, Angpt1, and Scf transcripts [21]. Downregulation of SCF and/or ANG-1 expression has also been described in MSCs from patients with AML [12] and MDS [16,17].

Furthermore, both CD146/MCAM (a perivascular marker of MSCs) and CD49e/ITGA5 (the main ligand for fibronectin) were upregulated in L-MSCs, as reported in patients with MDS [16] and primary myelofibrosis [42] and in mice with chemically induced leukemia [43]. Despite ITG5A upregulation in L-MSCs, extracellular deposition of fibronectin (its ligand) was comparable in L- and N-MSCs. An over-representation of the CD146^{pos} MSC subpopulation in leukemic BM may reflect changes in MSC distribution in favor of perisinusoidal sites [44] where reticular cells co-express CD271 and CD146 antigens [45]. The positive correlation between CD146 and CD49e expression levels is consistent with this hypothesis since increased alpha5
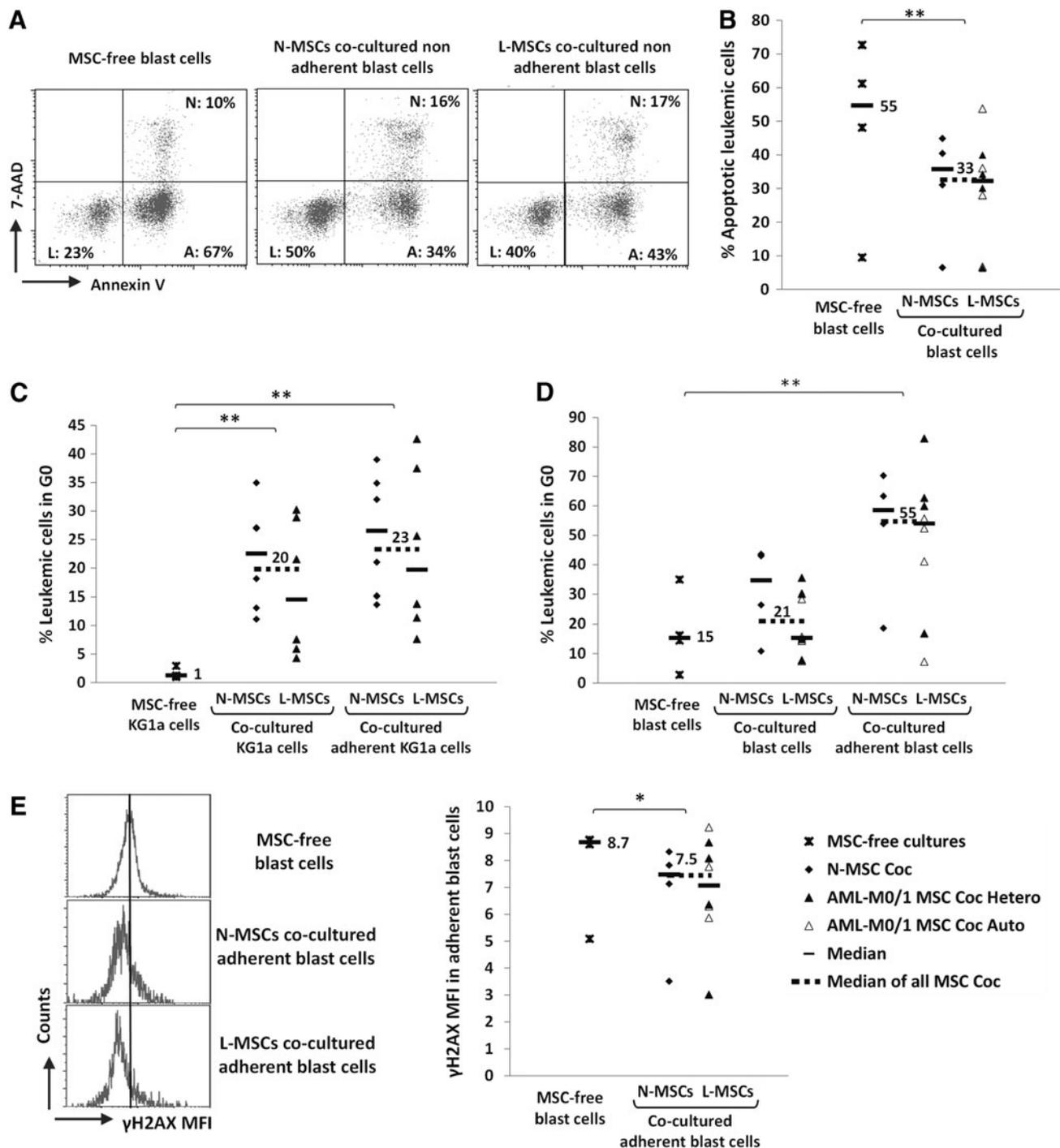
FIG. 7. L-MSCs and N-MSCs protect leukemic cells from apoptosis and promote their quiescence in a similar manner. Cocultures of KG1a cells or primary blast cells (AML-M0/1) with L-MSCs (AML-M0/1) or N-MSCs for 2–3 days. Blast cells were cocultured either with heterologous (Coc Hetero) or autologous (Coc Auto) L-MSCs. Leukemic cells (CD45^{pos} cell fraction) were analyzed by flow cytometry. For each experiment, one L-MSC coculture with KG1a cells ($n=6$) or primary blast cells ($n=8$) was matched with one N-MSC coculture with KG1a cells ($n=6$) or primary blast cells ($n=4$) and both compared with KG1a cells ($n=3$) and primary blast cells ($n=4$) cultured without MSCs. **(A)** Representative images of apoptosis quantification in primary blast cells cocultured or not with MSCs determined by Annexin V/7-AAD staining. **(B)** Individual percentages of apoptotic (AAD[neg] Annexin V[pos]) primary blast cells. **(C, D)** Cell cycle analysis after 7-AAD/Ki-67 staining. Quantification of KG1a **(C)** and primary blast **(D)** cells in G0 (7-AAD[low]/Ki-67^{neg}) cells. **(E)** Representative images of DNA double-strand break detection in primary blast cells cocultured or not with MSCs by anti-γH2AX staining **(E,** *left***)**; quantification of DNA double-strand breaks, as indicated by the MFIs of γH2AX staining, in adherent primary blast cells **(E,** *right***)**. *Crosses*, MSC-free cultures; *black diamonds*, cocultures with N-MSCs; *black triangles*, cocultures with heterologous L-MSCs; *empty triangles*, cocultures with autologous L-MSCs. *Horizontal bars* represent the medians. *$P < 0.05$; **$P < 0.01$.

integrin expression has been associated with pericyte differentiation [46]. In accordance with a report showing that leukemic proliferation in a mouse model can induce deficiency of osteoblastic cells [38], our study shows a concomitant lower expression of osteogenic (OCN, RUNX2) differentiation genes in L-MSCs, as reported in humans with MDS [17,47] and more recently in AML [12]. In addition to these data, our finding that CD146 levels in L-MSCs correlated with the degree of BM leukoblast infiltration argues for leukemia-induced changes in BM MSC distribution in favor of perisinusoidal sites at the expense of endosteal sites. The inverse correlation we observed between CD146 protein expression levels and age is consistent with a report showing in elderly people a decrease of the BM CD146^{pos} cell population in favor of CD146^{neg} MSCs [48].

Considering the phenotypic changes observed in L-MSCs, we investigated whether they were related to their growth capacities and senescence levels. Thus, prolonged PDT and decreased clonogenic potential were associated with a particular MSC phenotype, including lower expression of osteogenic (RUNX2) and chondrogenic (COL10A1) markers, as well as of the niche factors, THPO, CXCL12, and ANGPT1, and higher expression of BMP1, ITGA5, and JAG1. The latter gene (which encodes the protein Jagged 1) has been shown to be associated with breast cancer development [49] and involved in BM stroma-dependent AML induction [50] and chemoresistance [51]. In these conditions, the independent prognostic value of MSC PDT found in our study, which was negatively correlated with JAG1 gene expression, appears of particular interest. This must be compared with the higher Jagged 1 expression on L-MSCs than on N-MSCs, as previously reported [12,49]. Anyway, the direct involvement of Jagged 1 in L-MSC proliferation needs to be elucidated.

Likewise, senescence levels of L-MSCs (that increased with lower clonogenic potential) were associated with lower gene expression of RUNX2, COL10A1, and ANGPT1 and particularly of DICER1 and BMI1 whose expression levels were strongly correlated with each other. Our study extends to AML patients' DICER1 downregulation previously reported in MSCs from MDS patients [52]. Additionally, the inverse relationship between DICER1 or BMI1 expression and senescence levels in L-MSCs is consistent with the role of both factors recently shown to protect MSCs from senescence [53,54].

Finally, we evaluated whether L-MSC abnormalities had an effect on their supportive function on normal and leukemic hematopoiesis. The capacity to support normal hematopoiesis, assessed by Dexter-type long-term cultures, was comparable in L-MSCs (only from patients with AML-M0/1 for better homogeneity) and N-MSCs. These results were confirmed by the observation of HPC production by adherent layers and cobblestone area formation at week 5. Of note, L-MSC hematopoiesis-supporting activity was normal regardless of their proliferative capacity and despite lower VCAM-1 expression. Normal HPC production has also been reported in a previous study using immunoselected AML-MSCs [10], in contrast to other studies where different (sometimes suboptimal) culture conditions of MSCs were used [9,12,55]. Our findings are consistent with a very recent study in a murine model of AML indicating that BM microenvironment retains in vivo supporting activity of normal

hematopoiesis [56]. Normal supporting activity of MSCs from patients with hematological malignancies was also shown in CML [18], myeloma [57], and lymphoma [9], whereas impaired function has been reported in ALL [31,32], CLL [34], and particularly MDS [15–17,35,36,58].

N-MSCs are also known to protect leukemic cells (particularly in AML) from apoptosis, favor their chemoresistance, and induce their quiescence [3,4,59,60]. In this study, we show that L-MSCs and N-MSCs similarly decrease the levels of early and late apoptotic leukemic cells and increase the proportion of leukemic cells in G_0 associated with a slight decrease in DNA DSB levels. Moreover, when comparing the results of matched autologous and heterologous cocultures of L-MSCs and primary blast cells, we did not find any significant difference. Our data are in accordance with a very recent study in which rates of in vivo engraftment of primary blast cells were not different when previously cocultured on L-MSCs and N-MSCs [13].

To explain the normal supportive function of L-MSCs found in our work, the selection of MSC subsets is not totally excluded, possibly favored by our culture conditions, in which the use of FGF2-supplemented MSC medium is certainly not negligible. On another side, it is conceivable that properties of MSCs from de novo AML patients at the onset of their disease are quite different than those from patients with other chronic hematological disorders, such as MDS. In these diseases, the well-known, long-term, and stronger impairment of the stromal cell compartment in a chronic inflammatory context could even promote the leukemia emergence [61].

In conclusion, our study highlights some changes of the stromal cell compartment during AML cell expansion. They include proliferation deficiency, increased apoptosis, downregulation of several niche-related factors, and a tendency to exhibit a perivascular feature at the expense of the osteo-chondroblastic lineage. However, all these changes were not associated with altered MSC supporting function on normal and leukemic hematopoiesis in vitro. Finally, these findings suggest that the impairment of BM-derived MSCs observed at the onset of de novo AML does not play a special role in the leukemic process.

Acknowledgments

Author Disclosure Statement

No competing financial interests exist.

References

1. Ferrara F and C Schiffer. (2013). Acute myeloid leukaemia in adults. Lancet 381:484–495.
2. Dick JE. (2008). Stem cell concepts renew cancer research. Blood 112:4793–4807.
3. Garrido SM, FR Appelbaum, CL Willman and DE Banker. (2001). Acute myeloid leukemia cells are protected from spontaneous and drug-induced apoptosis by direct contact with a human bone marrow stromal cell line (HS-5). Exp Hematol 29:448–457.
4. Konopleva M, S Konoplev, W Hu, AY Zaritskey, BV Afanasiev and M Andreeff. (2002). Stromal cells prevent apoptosis of AML cells by up-regulation of anti-apoptotic proteins. Leukemia 16:1713–1724.
5. Costello RT, F Mallet, B Gaugler, D Sainty, C Arnoulet, JA Gastaut and D Olive. (2000). Human acute myeloid leukemia CD34+/CD38− progenitor cells have decreased sensitivity to chemotherapy and Fas-induced apoptosis, reduced immunogenicity, and impaired dendritic cell transformation capacities. Cancer Res 60:4403–4411.
6. Dennis JE and P Charbord. (2002). Origin and differentiation of human and murine stroma. Stem Cells 20:205–214.
7. Caplan AI. (1991). Mesenchymal stem cells. J Orthop Res 9:641–650.
8. Prockop DJ. (1997). Marrow stromal cells as stem cells for nonhematopoietic tissues. Science 276:71–74.
9. Zhao ZG, Y Liang, K Li, WM Li, QB Li, ZC Chen and P Zou. (2007). Phenotypic and functional comparison of mesenchymal stem cells derived from the bone marrow of normal adults and patients with hematologic malignant diseases. Stem Cells Dev 16:637–648.
10. Campioni D, F Lanza, S Moretti, M Dominici, M Punturieri, S Pauli, T Hofmann, E Horwitz and GL Castoldi. (2003). Functional and immunophenotypic characteristics of isolated CD105(+) and fibroblast(+) stromal cells from AML: implications for their plasticity along endothelial lineage. Cytotherapy 5:66–79.
11. Mayani H. (1996). Composition and function of the hemopoietic microenvironment in human myeloid leukemia. Leukemia 10:1041–1047.
12. Geyh S, M Rodríguez-Paredes, P Jäger, C Khandanpour, R-P Cadeddu, J Gutekunst, CM Wilk, R Fenk, C Zilkens, et al. (2016). Functional inhibition of mesenchymal stromal cells in acute myeloid leukemia. Leukemia 30:683–691.
13. Kim JA, JS Shim, GY Lee, HW Yim, TM Kim, M Kim, SH Leem, JW Lee, CK Min and IH Oh. (2015). Micro-environmental remodeling as a parameter and prognostic factor of heterogeneous leukemogenesis in acute myelogenous leukemia. Cancer Res 75:2222–2231.
14. Chandran P, Y Le, Y Li, M Sabloff, J Mehic, M Rosu-Myles and DS Allan. (2015). Mesenchymal stromal cells from patients with acute myeloid leukemia have altered capacity to expand differentiated hematopoietic progenitors. Leuk Res 39:486–493.
15. Zhao ZG, W Xu, HP Yu, BL Fang, SH Wu, F Li, WM Li, QB Li, ZC Chen and P Zou. (2012). Functional characteristics of mesenchymal stem cells derived from bone marrow of patients with myelodysplastic syndromes. Cancer Lett 317:136–143.
16. Ferrer RA, M Wobus, C List, R Wehner, C Schönefeldt, B Brocard, B Mohr, M Rauner, M Schmitz, et al. (2013). Mesenchymal stromal cells from patients with myelodyplastic syndrome display distinct functional alterations that are modulated by lenalidomide. Haematologica 98: 1677–1685.
17. Geyh S, S Oz, RP Cadeddu, J Fröbel, B Brückner, A Kündgen, R Fenk, I Bruns, C Zilkens, et al. (2013). Insufficient stromal support in MDS results from molecular and functional deficits of mesenchymal stromal cells. Leukemia 27:1841–1851.
18. Jootar S, N Pornprasertsud, S Petvises, B Rerkamnuaychoke, S Disthabanchong, S Pakakasama, A Ungkanont and S Hongeng. (2006). Bone marrow derived mesenchymal stem cells from chronic myeloid leukemia t(9;22) patients are devoid of Philadelphia chromosome and support cord blood stem cell expansion. Leuk Res 30:1493–1498.
19. Estrada-González PK, L Gómez-Ceja, JJ Montesinos, H Mayani, A Chávez-González, L Meillón, N Delgado, E Sánchez-Nava and E Flores-Figueroa. (2014). Decreased frequency, but normal functional integrity of mesenchymal stromal cells derived from untreated and Imatinib-treated chronic myeloid leukemia patients. Leuk Res 38:594–600.
20. Colmone A, M Amorim, AL Pontier, S Wang, E Jablonski and DA Sipkins. (2008). Leukemic cells create bone marrow niches that disrupt the behavior of normal hematopoietic progenitor cells. Science 322:1861–1865.
21. Hanoun M, D Zhang, T Mizoguchi, S Pinho, H Pierce, Y Kunisaki, J Lacombe, SAA Armstrong, U Dührsen and PSS Frenette. (2014). Acute myelogenous leukemia-induced sympathetic neuropathy promotes malignancy in an altered hematopoietic stem cell niche. Cell Stem Cell 15:1–11.
22. Hertenstein B, L Hambach and A Bacigalupo. (2005). Development of leukemia in donor cells after allogeneic stem cell transplantation—a survey of the European Group for Blood and Marrow Transplantation (EBMT). Haematologica 90:969–975.
23. Sala-Torra O, C Hanna, MR Loken, MED Flowers, M Maris, PA Ladne, JR Mason, D Senitzer, R Rodriguez, et al. (2006). Evidence of donor-derived hematologic malignancies after hematopoietic stem cell transplantation. Biol Blood Marrow Transplant 12:511–517.
24. Walkley CR, JM Shea, NA Sims, LE Purton and SH Orkin. (2007). Rb regulates interactions between hematopoietic stem cells and their bone marrow microenvironment. Cell 129:1081–1095.
25. Walkley CR, GH Olsen, S Dworkin, SA Fabb, J Swann, GA McArthur, SV Westmoreland, P Chambon, DT Scadden and LE Purton. (2007). A microenvironment-induced myeloproliferative syndrome caused by retinoic acid receptor gamma deficiency. Cell 129:1097–1110.
26. Raaijmakers MH, S Mukherjee, S Guo, S Zhang, T Kobayashi, JA Schoonmaker, BL Ebert, F Al-Shahrour, RP Hasserjian, et al. (2010). Bone progenitor dysfunction induces myelodysplasia and secondary leukaemia. Nature 464:852–857.
27. Herault O, J Domenech, M Degenne, JL Bremond, L Sensebe, MC Bernard, C Binet and P Colombat. (1998). All-trans-retinoic acid up-regulates CD38 but not c-Kit antigens on human marrow CD34+ cells without recruitment into cell cycle. Br J Haematol 103:343–350.
28. Herault O, P Colombat, J Domenech, M Degenne, JL Bremond, L Sensebe, MC Bernard and C Binet. (1999). A rapid single-laser flow cytometric method for discrimination of early apoptotic cells in a heterogenous cell population. Br J Haematol 104:530–537.
29. Humar B, H Müller and R Scott. (2001). Cell cycle dependent DNA break increase in ataxia telangiectasia lymphoblasts after radiation exposure. Mol Pathol 347–350.

30. Dominici M, K Le Blanc, I Mueller, I Slaper-Cortenbach, F Marini, D Krause, R Deans, A Keating, D Prockop and E Horwitz. (2006). Minimal criteria for defining multipotent mesenchymal stromal cells. The International Society for Cellular Therapy position statement. Cytotherapy 8:315–317.

31. Conforti A, S Biagini, F Del Bufalo, P Sirleto, A Angioni, N Starc, G Li Pira, F Moretta, A Proia, et al. (2013). Biological, functional and genetic characterization of bone marrow-derived mesenchymal stromal cells from pediatric patients affected by acute lymphoblastic leukemia. PLoS One 8:e76989.

32. Vicente López Á, MN Vázquez García, GJ Melen, A Entrena Martínez, I Cubillo Moreno, J García-Castro, MR Orellana and AGZ González. (2014). Mesenchymal stromal cells derived from the bone marrow of acute lymphoblastic leukemia patients show altered BMP4 production: correlations with the course of disease. PLoS One 9:e84496.

33. Pontikoglou C, MC Kastrinaki, M Klaus, C Kalpadakis, P Katonis, K Alpantaki, GA Pangalis and HA Papadaki. (2013). Study of the quantitative, functional, cytogenetic, and immunoregulatory properties of bone marrow mesenchymal stem cells in patients with B-cell chronic lymphocytic leukemia. Stem Cells Dev 22:1329–1341.

34. Janel A, F Dubois-Galopin, C Bourgne, J Berger, K Tarte, N Boiret-Dupré, S Boisgard, P Verrelle, P Déchelotte, O Tournilhac and MG Berger. (2014). The chronic lymphocytic leukemia clone disrupts the bone marrow microenvironment. Stem Cells Dev 23:2972–2982.

35. Aanei CM, P Flandrin, FZ Eloae, E Carasevici, D Guyotat, E Wattel and L Campos. (2012). Intrinsic growth deficiencies of mesenchymal stromal cells in myelodysplastic syndromes. Stem Cells Dev 21:1604–1615.

36. Pavlaki K, CG Pontikoglou, A Demetriadou, AK Batsali, A Damianaki, E Simantirakis, M Kontakis, A Galanopoulos, I Kotsianidis, M-C Kastrinaki and HA Papadaki. (2014). Impaired proliferative potential of bone marrow mesenchymal stromal cells in patients with myelodysplastic syndromes is associated with abnormal WNT signaling pathway. Stem Cells Dev 23:1568–1581.

37. Aoyagi M, S Furusawa, K Waga, S Tsunogake and H Shishido. (1994). Suppression of normal hematopoiesis in acute leukemia: effect of leukemic cells on bone marrow stromal cells and hematopoietic progenitor cells. Intern Med 33:288–295.

38. Frisch BJ, JM Ashton, L Xing, MW Becker, CT Jordan and LM Calvi. (2012). Functional inhibition of osteoblastic cells in an in vivo mouse model of myeloid leukemia. Blood 119:540–550.

39. Bowers M, B Zhang, Y Ho, P Agarwal, C-C Chen and R Bhatia. (2015). Osteoblast ablation reduces normal long-term hematopoietic stem cell self-renewal but accelerates leukemia development. Blood 125:2678–2688.

40. Dvořáková M, V Karafiát, P Pajer, E Kluzáková, K Jarkovská, S Peková, L Krutílková, M Dvořák, M Dvorakova, et al. (2013). DNA released by leukemic cells contributes to the disruption of the bone marrow microenvironment. Oncogene 32:5201–5209.

41. Ho JH, YF Chen, WH Ma, TC Tseng, MH Chen and OK Lee. (2011). Cell contact accelerates replicative senescence of human mesenchymal stem cells independent of telomere shortening and p53 activation: roles of Ras and oxidative stress. Cell Transpl 20:1209–1220.

42. Tripodo C, A Di Bernardo, MP Ternullo, C Guarnotta, R Porcasi, S Ingrao, U Gianelli, E Boveri, E Iannitto, G Franco and AM Florena. (2009). CD146(+) bone marrow osteoprogenitors increase in the advanced stages of primary myelofibrosis. Haematologica 94:127–130.

43. Basak P, S Chatterjee, P Das, M Das, JA Pereira, RK Dutta, M Chaklader, S Chaudhuri and S Law. (2010). Leukemic stromal hematopoietic microenvironment negatively regulates the normal hematopoiesis in mouse model of leukemia. Chin J Cancer 29:969–979.

44. Sacchetti B, A Funari, S Michienzi, S Di Cesare, S Piersanti, I Saggio, E Tagliafico, S Ferrari, PG Robey, et al. (2007). Self-renewing osteoprogenitors in bone marrow sinusoids can organize a hematopoietic microenvironment. Cell 131:324–336.

45. Tormin A, O Li, JC Brune, S Walsh, B Schutz, M Ehinger, N Ditzel, M Kassem and S Scheding. (2011). CD146 expression on primary nonhematopoietic bone marrow stem cells is correlated with in situ localization. Blood 117: 5067–5077.

46. Kale S. (2004). Microarray analysis of in vitro pericyte differentiation reveals an angiogenic program of gene expression. FASEB J 19:270–271.

47. Fei C, Y Zhao, S Gu, J Guo, X Zhang, X Li and C Chang. (2014). Impaired osteogenic differentiation of mesenchymal stem cells derived from bone marrow of patients with lower-risk myelodysplastic syndromes. Tumour Biol 35:4307–4316.

48. Maijenburg MW, M Kleijer, K Vermeul, EPJ Mul, FPJ van Alphen, CE van der Schoot and C Voermans. (2012). The composition of the mesenchymal stromal cell compartment in human bone marrow changes during development and aging. Haematologica 97:179–183.

49. Reedijk M, S Odorcic, L Chang, H Zhang, N Miller, DR McCready, G Lockwood and E Sean. (2005). High-level coexpression of JAG1 and NOTCH1 is observed in human breast cancer and is associated with poor overall survival. Cancer Res 65:8530–8537.

50. Kode A, JS Manavalan, I Mosialou, G Bhagat, CV Rathinam, N Luo, H Khiabanian, A Lee, V V Murty, et al. (2014). Leukaemogenesis induced by an activating β-catenin mutation in osteoblasts. Nature 506:240–244.

51. Takam Kamga P, G Bassi, A Cassaro, M Midolo, M Di Trapani, A Gatti, R Carusone, F Resci, O Perbellini, et al. (2016). Notch signalling drives bone marrow stromal cell-mediated chemoresistance in acute myeloid leukemia. Oncotarget 7:21713–21727.

52. Santamaria C, S Muntion, B Roson, B Blanco, O Lopez-Villar, S Carrancio, FM Sanchez-Guijo, M Diez-Campelo, S Alvarez-Fernandez, et al. (2012). Impaired expression of DICER, DROSHA, SBDS and some microRNAs in mesenchymal stromal cells from myelodysplastic syndrome patients. Haematologica 97:1218–1224.

53. Zhao Y, D Wu, C Fei, J Guo, S Gu, Y Zhu, F Xu, Z Zhang, L Wu, X Li and C Chang. (2014). Down-regulation of Dicer1 promotes cellular senescence and decreases the differentiation and stem cell-supporting capacities of mesenchymal stromal cells in patients with myelodysplastic syndrome. Haematologica 100:194–204.

54. Lee JY, KR Yu, HS Kim, I Kang, JJ Kim, BC Lee, SW Choi, JH Shin, Y Seo and KS Kang. (2016). BMI1 inhibits senescence and enhances the immunomodulatory properties of human mesenchymal stem cells via the direct suppression of MKP-1/DUSP1. Aging (Albany NY) 8:1670–1689.

55. Sparrow RL, E O'Flaherty, TM Blanksby, J Szer and MB Van Der Weyden. (1997). Perturbation in the ability of bone marrow stroma from patients with acute myeloid

leukemia but not chronic myeloid leukemia to support normal early hematopoietic progenitor cells. Leuk Res 21:29–36.

56. Boyd AL, CJ V. Campbell, CI Hopkins, A Fiebig-Comyn, J Russell, J Ulemek, R Foley, B Leber, A Xenocostas, et al. (2014). Niche displacement of human leukemic stem cells uniquely allows their competitive replacement with healthy HSPCs. J Exp Med 211:1925–1935.

57. Arnulf B, S Lecourt, J Soulier, B Ternaux, MN Lacassagne, A Crinquette, J Dessoly, AK Sciaini, M Benbunan, et al. (2007). Phenotypic and functional characterization of bone marrow mesenchymal stem cells derived from patients with multiple myeloma. Leukemia 21:158–163.

58. Tennant GB, V Walsh, LN Truran, P Edwards, KI Mills and AK Burnett. (2000). Abnormalities of adherent layers grown from bone marrow of patients with myelodysplasia. Br J Haematol 111:853–862.

59. Jacamo R, Y Chen, Z Wang, W Ma, M Zhang, EL Spaeth, Y Wang, VL Battula, PY Mak, et al. (2014). Reciprocal leukemia-stroma VCAM-1/VLA-4-dependent activation of NF- k B mediates chemoresistance. Blood 123:2691–2702.

60. Ramasamy R, EW Lam, I Soeiro, V Tisato, D Bonnet and F Dazzi. (2007). Mesenchymal stem cells inhibit proliferation and apoptosis of tumor cells: impact on in vivo tumor growth. Leukemia 21:304–310.

61. Zambetti NA, Z Ping, S Chen, KJG Kenswil, MA Mylona, MA Sanders, RM Hoogenboezem, EMJ Bindels, MN Adisty, et al. (2016). Mesenchymal inflammation drives genotoxic stress in hematopoietic stem cells and predicts disease evolution in human pre-leukemia. Cell Stem Cell 19:613–627.

Address correspondence to:
Jorge Domenech, MD, PhD
Service d'Hématologie Biologique
CHRU de Tours and CNRS UMR 7292
2 Boulevard Tonnellé
Tours Cedex 9, 37044
France

E-mail: jorge.domenech@univ-tours.fr